

# RSC Advances



This is an *Accepted Manuscript*, which has been through the Royal Society of Chemistry peer review process and has been accepted for publication.

*Accepted Manuscripts* are published online shortly after acceptance, before technical editing, formatting and proof reading. Using this free service, authors can make their results available to the community, in citable form, before we publish the edited article. This *Accepted Manuscript* will be replaced by the edited, formatted and paginated article as soon as this is available.

You can find more information about *Accepted Manuscripts* in the [Information for Authors](#).

Please note that technical editing may introduce minor changes to the text and/or graphics, which may alter content. The journal's standard [Terms & Conditions](#) and the [Ethical guidelines](#) still apply. In no event shall the Royal Society of Chemistry be held responsible for any errors or omissions in this *Accepted Manuscript* or any consequences arising from the use of any information it contains.

# Controllable synthesis and growth mechanism of dual size distributed PbSe quantum dots

Ruifeng Li<sup>a</sup>, Zhenyu Ye<sup>a</sup>, Weiguang Kong<sup>a</sup>, and Huizhen Wu<sup>\*a</sup>, Xing Lin<sup>b</sup> and Wei Fang<sup>b</sup>

a) Department of Physics and State Key Laboratory of Silicon Materials, Zhejiang University, Hangzhou, Zhejiang 310027, P.R. China \*Email: hzww@zju.edu.cn

b) Department of Optical engineering, Zhejiang University, Hangzhou, Zhejiang 310027, P.R. China

**Abstract:** To understand the fundamental science of nanocrystal growth, controllable synthesis and growth mechanism of dual size distributed PbSe quantum dots (QDs) are studied. The characterizations of high-resolution transmission electron microscope (HR-TEM) and photoluminescence (PL) unambiguously demonstrate the dual size distribution of PbSe QDs. Thermodynamic stability of small QDs is confirmed by a controllable synthesis of temperature variation and kinetic perturbation with successive injection of precursors, suggesting a possible mechanism that a chemical-potential well may lead to the size separation. The control of growth temperature plays an important role in the realization of dual size distributed PbSe QDs. Further study of temporal evolution demonstrates the size refocusing of QDs at a higher temperature. Both kinetic perturbation and thermodynamic perturbation could facilitate QDs to overcome the potential barrier. Understanding this mechanism is of significance for the controllable synthesis and applications of PbSe QDs.

## 1. Introduction

Lead chalcogenide nanocrystal quantum dots (QDs) have attracted continuous scientific and industrial interests for the extraordinary optical and electrical properties. In particular,

PbSe QDs, with a large exciton Bohr radius (46nm) and narrow bulk band-gap (0.278eV at 300K), have capability to tune luminescent wavelength from near-infrared to visible, covering an important spectral range that have potential applications in telecommunication<sup>1</sup>, photovoltaic devices<sup>2,3</sup> and bio-imaging<sup>4</sup>. For instance, PbSe QDs have an effect of multiple exciton generation (MEG), which can provide an opportunity to increase power conversion efficiency of solar cells beyond the Shockley-Queisser thermodynamic limit.<sup>5,6</sup> Particularly, ultra-small PbSe QDs are getting more attention for its excellent performance derived from the strong quantum confinement. Recently, ultra-small PbSe QDs fabricated for Schottky solar cells shows a device efficiency of 4.57% on the size of 2.3nm, where the larger band-gap of the QDs leads to higher open-circuit voltages.<sup>7</sup> Furthermore, high quantum efficiency of light emitting was also acquired from the study of PbSe magic size clusters, which allows biological imaging at a window from 700nm to 1000nm, where organic dyes emit poorly.<sup>8</sup> Hence, synthesis and understanding of physical properties of ultra-small PbSe QDs are well worth studied, while the synthesis of PbSe QDs as small as 2~4 nm will benefit the photovoltaic and biological applications.

A hot-injection approach to synthesize PbSe QDs was initially introduced by Murray and co-workers in 2001.<sup>9</sup> Typically, lead oleate and n-trioctylphosphine selenide were used as the precursor of Pb and Se, respectively. The reaction was carried out in the non-coordinating solvent (1-octadecene), which was developed by Yu and co-workers.<sup>10</sup> The ultra-small PbSe magic-sized nano-clusters were also synthesized under a similar approach but at room temperature, which could be carried out even in air for hours.<sup>8</sup> One-pot non-injection method with high chemical yields was also utilized to synthesize ultra-small PbSe QDs.<sup>11</sup> In these

synthesis approaches, the formation of QDs undergoes the nucleation and growth process, where the thermodynamic and kinetic factors exert significant influence on the reaction. However, how these factors affect the reaction has not been thoroughly understood.

Moreover, few studies have reported the bimodal or multi-modal size distribution of IV-VI QDs, where the mechanism of this phenomenon probably provides an opportunity to understand the role of thermodynamic and kinetic factors on nanocrystal growth. In general, synthesis of QDs for high quality and monodispersity undergoes a temporally discrete nucleation event followed by relatively rapid growth from monomers and finally slower and long-time growth by Ostwald ripening.<sup>12</sup> This standard model simply demonstrates a continuous growth process. Recent study of magic size CdSe QDs has reported individual emission peaks which stem from a non-continuous growth process.<sup>13</sup> Thus by varying and control of the synthetic conditions, non-continue growth may occur. It offers a possible approach to achieve desired size distribution.

Herein, it is the first time that dual size distributed PbSe QDs are directly observed. A typical hot-injection method<sup>10, 14, 15</sup> was applied in our synthesis of dual-size distributed PbSe QDs. In the general approach of synthesis, the reaction is always under a single temperature control. Differently, dual-size distributed PbSe QDs were realized by varying the growth temperature when the nanocrystals just started to grow at the early stage right after a nucleation event. High-resolution transmission electron microscope (HR-TEM) and photoluminescence (PL) provide a strong evidence of dual-size distribution of the PbSe QDs. In order to gain insight into the nature of the dual-size distribution, we then performed a kinetic perturbation experiment to identify the thermodynamic stability of our QDs. Moreover,

the temporal evolution from dual size distribution to uniform size distribution is probed via thermodynamic perturbation. Thereby, both kinetic perturbation and thermodynamic perturbation are found to facilitate QDs overcoming the chemical-potential barrier. We conclude these findings with a schematic theoretical description. The study of the dual size distribution phenomena offers a good opportunity to get insight into the fundamental science of nanocrystal growth. Thus, understanding the growth mechanism may benefit both synthesis and application of PbSe QDs.

## 2. Experiments

### 2.1 Chemicals

Chemicals used are commercially available from Alfa Aesar (or otherwise specified) and were used as received: Lead oxide (PbO; 99.95%), selenium powder (Se; 99.999%), Oleic acid (OA; 90%), 1-octadecane (ODE; 90%) and trioctylphosphine (TOP; 90%). Toluene (99.5%), methanol (99.5%), hexane (97%) and acetone (99.5%) were purchased from Sinopharm.

### 2.2 Synthesis of dual size distributed PbSe QDs

A 1.0 M solution of trioctylphosphine-selenide (TOP-Se) was prepared by dissolving selenium powders in TOP in a flask under an N<sub>2</sub> atmosphere. The flask was then put in an ultrasonic device to make the selenium powder fully dissolved. Lead oxide (0.892 g, 4 mmol), oleic acid (2 mL, 6 mmol), and ODE (10 mL) were loaded into a three-neck flask and heated to 100 °C to remove air and water under N<sub>2</sub> flow for an hour. Clear solution was achieved after the flask was heated to 150 °C. 4mL of 1.0 M TOP-Se was quickly injected into the reaction flask at different temperatures to synthesize specific QDs. The colour of the mixture

changed from nearly transparent to dark brown in 30 seconds after Se-precursor injection, indicating the nucleation and growth of PbSe QDs. To achieve dual-size distributed PbSe QDs, the heater was quickly removed after 30 seconds. To study the effect of different injection temperatures, the solution was naturally cooled down to room temperature in a rate of  $\sim 15^{\circ}\text{C}/\text{min}$ . To perform the study of thermodynamic stability, solution was firstly cooled down to  $70^{\circ}\text{C}$  as fast as  $\sim 40^{\circ}\text{C}/\text{min}$  by an ice-water bath and was kept  $70^{\circ}\text{C}$  for different reaction time. Successive 1mL of Se-precursors was then injected to initiate the growth again. Another temporal evolution experiments were carried out by a reaction started with a TOP-Se injection at  $130^{\circ}\text{C}$ . These samples were extracted twice (3min and 5min) with a cooling rate of  $\sim 15^{\circ}\text{C}/\text{min}$  to achieve dual size distributed PbSe QDs. Then the rest of the solution was set to  $110^{\circ}\text{C}$  for the further growth and ripening. Unreacted precursors and excess ligands were extracted by adding methanol and toluene in a ratio of 3:1. The extraction procedure was repeated by 3 times. The QDs were then centrifuged by acetone and hexane in 4000 r/min. Finally, the QDs were re-dispersed in hexane for characterizations.

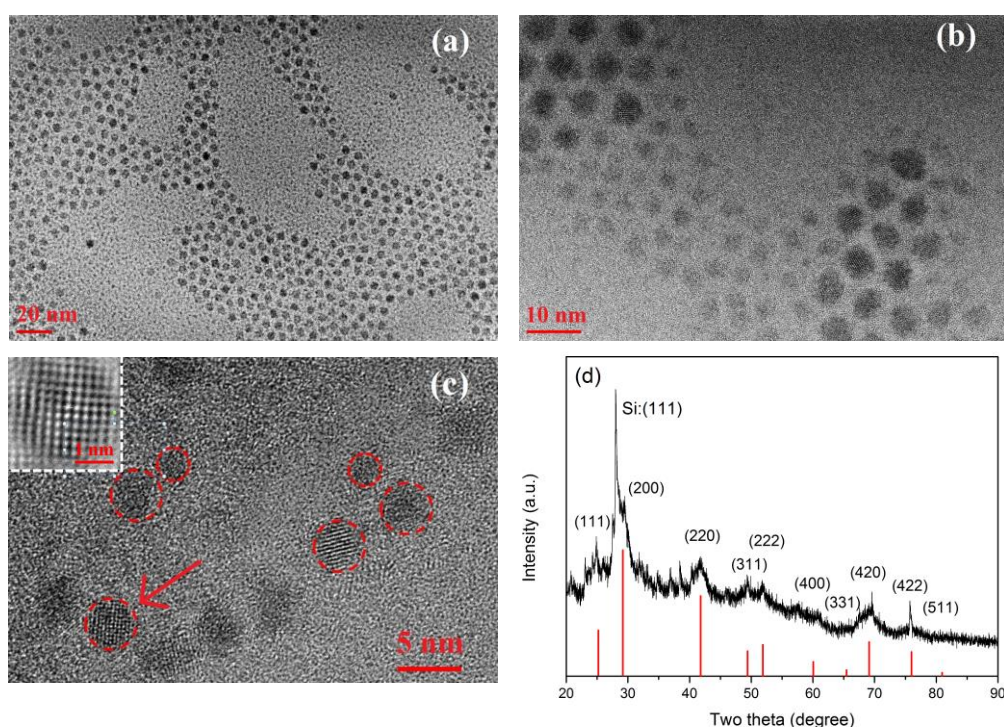
### 2.3 Characterizations

All samples were immediately purified after they were taken out from the reaction flask. Sample preparations were quickly completed by spin-coating PbSe QDs on a silicon substrate to form a solid state film. Samples prepared for XRD were performed via a thick coating of PbSe QDs on a silicon substrate to acquire high intensity and signal to noise ratio. Some of the PL measurements were performed by two systems on account of experimental limitations from gratings and detectors. The near-infrared signals ( $>1100\text{nm}$ ) were collected by an InAs detector on an Edinburgh FLS920 system equipped with an EPL405 laser diode. Spectra

ranging from 600nm to 1100nm were measured by an EMCCD from Princeton Instrument. Absorption spectra were performed on a Shimadzu UV-3600 UV-VIS System. HR-TEM measurements were performed by a Tecnai G2 F20 system.

### 3. Results and discussion

#### 3.1 Morphology and crystalline structure



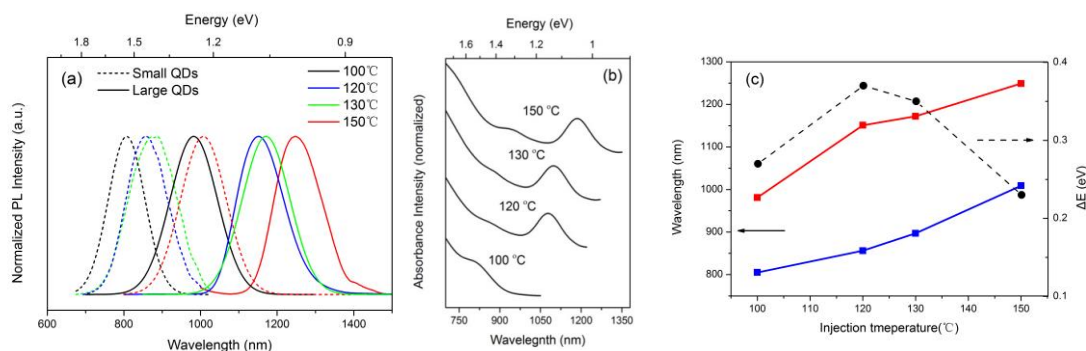
**Fig.1.** (a,b,c) The HR-TEM images of dual size distributed PbSe QDs with 20\10\5 nm scale, the inset of Fig.1.(c) displays an FFT transformed pattern of PbSe QDs. (d) The XRD pattern of PbSe QDs.

Fig.1 (a)(b)(c) present the HR-TEM images of the dual size distributed PbSe QDs, which are direct evidences that both the large and small QDs coexist. The inset of Fig.1(c) is the FFT transformed pattern of the HR-TEM image. The atoms and lattice structure are well observable. A d-spacing of 0.62nm is determined, which is in accordance with previous data of bulk PbSe powder. The image of HR-TEM shows that only single crystallized QDs with

regular spherical shapes are observed, indicating that the oriented attachment could be excluded as it always results in a formation of irregular shapes like nano rods or nano sheets.

Fig.1 (d) shows the XRD pattern of the PbSe QDs which were spin-coated on a silicon substrate. The peaks are well matched with the rock-salt structure of PbSe crystal (JCPDS No. 01-078-1903). A narrow and sharp peak at 28 degree originates from (111) plane of Si while the nearby 29 degree is determined to be (200) plane of PbSe QDs. The XRD pattern shows a highly crystallized structure, which coincides with the HR-TEM result.

### 3.2 Optical evidences of dual size distributed PbSe QDs



**Fig.2.** (a) PL spectra of dual emissions with different injection temperatures. (b) Corresponding absorption spectra of the PbSe QDs. (c) Emission peak positions as well as energy gaps (black dot) between the small QDs (blue square) and large QDs (red square) of the four samples versus injection temperatures.

Herein, the dual emissions of PL spectra correspond to the samples of different injection temperatures (100 °C, 120 °C, 130 °C, and 150 °C). The solutions were naturally cooled down to room temperature in a rate of  $\sim 15$  °C/min. The dual emissions of PbSe QDs are shown in Fig.2 (a), which demonstrates the existence of dual-size distributed PbSe QDs. The PL peaks were extracted from two systems and fitted by a Gaussian function for the limitations. The solid lines represent the large PbSe QDs while the dash lines represent the small QDs. We assumed

that QDs may have suffered some stable status during the growth of the decreasing temperature, where the growth of smaller QDs are more tempted to suspend while the larger QDs keep growing. Then the size distributions of PbSe QDs were separated. Optical absorption spectra of the samples are shown in Fig.2 (b). However, compared with the PL spectra, the absorption peaks overlap each other, thus being difficult to estimate QDs sizes and size distribution directly from the absorption spectra. (See S1 in **supporting information**)

**Table 1.** Peaks of dual emissions of PbSe QDs

	100°C	120°C	130°C	150°C
Small QDs (nm)	805	856	879	1009
Large QDs (nm)	981	1151	1172	1249
$\Delta E$ (eV)	0.27	0.37	0.35	0.23

To verify the existence of dual size distribution, the analysis of peak positions and energy gaps are given in Table 1 and Fig.1 (c). Smaller QDs are attributed to the shorter wavelength with larger band-gaps, while the larger QDs are attributed to the longer wavelength with smaller band-gaps, which are derived from the size-dependent quantum confinement in nanostructures. Apart from the size-dependent quantum confinement effect that determine the PL properties in our systems, other important features for small-size nanocrystals such as surface-related effects were described in the literature.<sup>16</sup> Here, the peaks of both small and large QDs shift to longer wavelength with increasing injection temperature. In general, after a rapid nucleation event at a moderate to high temperature (100°C-150°C for

IV-VI QDs), higher reaction temperature always yields larger average sizes of QDs. However, the energy gaps ( $\Delta E$ ) between the two emission peaks do not increase with temperature in monotone. Moreover, our tight-binding calculation (see S2 in **supporting information**) reveal that the energy gaps between  $1P_h-1P_e$  and  $1S_h-1S_e$  transitions of PbSe QDs are larger than the energy gaps between two emission peaks on corresponding sizes, suggesting that the two emission peaks originate from the dual size distributed QDs, other than the two energy transitions of one-size QDs ( $1S_h-1S_e$  and  $1P_h-1P_e$ ).<sup>17, 18</sup> Evidently, distinct and independent luminescent emissions of both large and small QDs are observed in each group of QDs, which means the dual-size distribution of QDs were obtained in each reaction.

### 3.3 Thermodynamic stability and kinetic perturbation of QDs

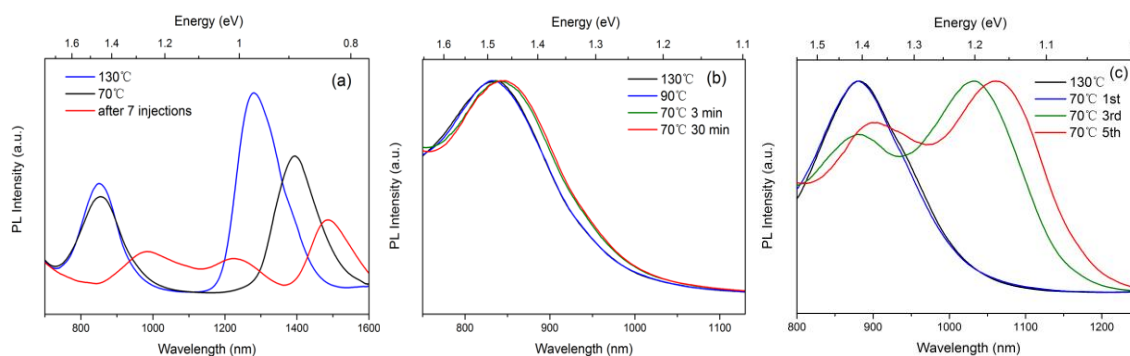


**Fig.3.** (a) PL spectra of PbSe QDs taken from 130°C/70°C when temperature was decreasing and QDs taken after 7 injections of precursors at 70°C. (b) PL spectra of small PbSe QDs when temperature was decreasing from 130°C to 70°C as well as temperature was kept for 30 minutes at 70°C. (c) PL spectra of QDs taken from the 1<sup>st</sup>, 3<sup>rd</sup> and 5<sup>th</sup> injection of precursors at 70°C.

In general, the growth of PbSe QDs is performed at a certain high temperature. When the growth temperature decreases to 70°C rapidly, the thermodynamic stability of small QDs may be a key factor for the size separation. To verify the stability of small QDs, we firstly take

aliquots from the reaction with a fast cooling rate ( $\sim 40^\circ\text{C}/\text{min}$ ). Peaks located around 850nm represent the PL emissions of small QDs while the longer wavelengths represent the larger QDs in Fig 3(a). In this case, the peak positions of small QDs are hardly shift, while larger QDs shifts more obviously ( $>100\text{nm}$ ). When sufficient precursors were added, after 7 injections, the QDs even developed into a multi-modal distribution.

For a better comprehension of the thermodynamic stability of small QDs, further studies of both temperature variation and kinetic perturbation were carried out. Aliquots were taken from the reaction to monitor the process. PL emissions in Fig.3(b) show that the emissions of small QDs hardly shift both when temperature was decreasing to  $70^\circ\text{C}$  as well as temperature was kept at  $70^\circ\text{C}$  for 30 minutes, which indicates that the growth are temporarily suspended. However, when kinetic perturbation is performed with injecting precursors (TOP-Se) to the reaction, the monomer concentration increases, which activates the growth again (shown in Fig.3(c)).

It is of great interest to understand the mechanism of suspension and restart of the growth. In a classic growth mechanism, nanocrystals grow continuously after the particles reach a certain radius (the critical size). However, the thermodynamic stability of QDs probably stems from the chemical-potential well during growth. When QDs fall into the chemical-potential well, as the temperature being dropped to  $70^\circ\text{C}$ , the growth will be suspended to retain the QDs in a certain size. In scope of the kinetic process on particle surface, monomers dynamically bind and unbind to the particle. However, when particle falls into the chemical-potential well, the binding and unbinding rates of monomers are temporarily balanced, which means the growth is suspended. On the other hand, monomers tend to unbind

when the size is slightly larger than this certain size. Only when sufficient energy is supplied, like the injection of successive monomers, can the particle overcome the potential barrier and continue to grow.

### 3.4 Thermodynamic perturbation and size refocusing of QDs

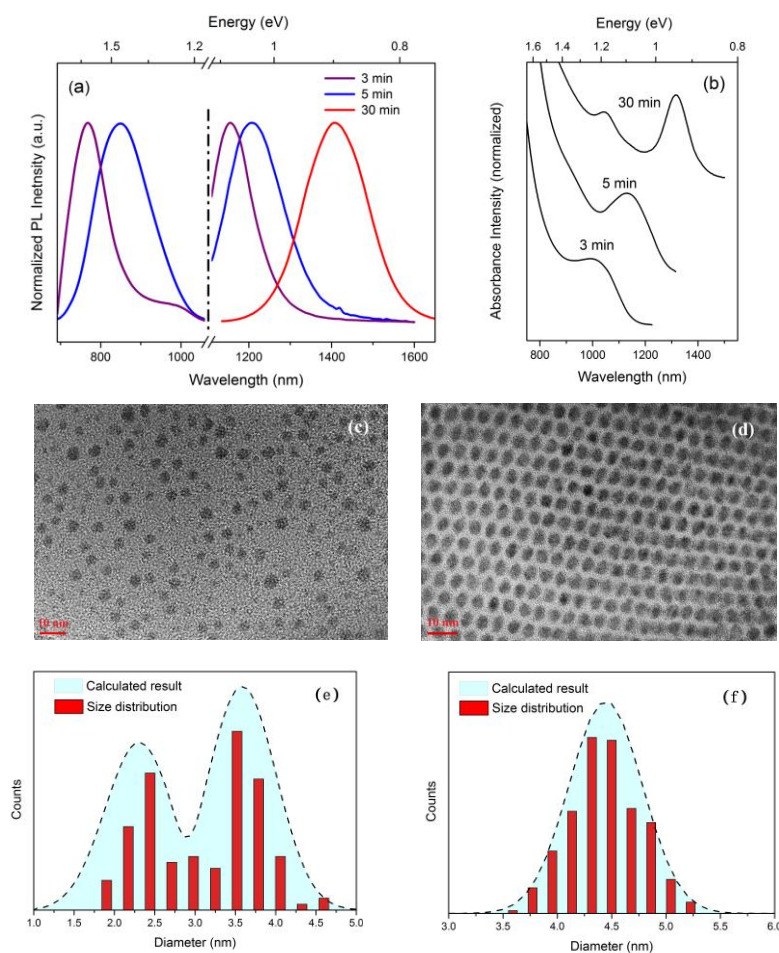


**Fig.4.** (a) PL spectra of the PbSe QDs with different reaction time. (b) Corresponding absorption spectra. (c) (d): HR-TEM images of the PbSe QDs. (e) (f): Histogram of size distributions and fittings.

The temporal evolutions demonstrate the size separation during the reaction with a naturally decreasing temperature and size refocusing under thermodynamic perturbation with higher temperature. PL and absorption spectra are illustrated in Fig.4 (a) and (b), respectively.

The purple lines represent a sample that was extracted from the reaction at 3 min during cooling, while the blue lines represent the reaction at 5 min. The emission with single peak (red line) corresponds to a further growth and ripening for 30 minutes, which shows a size refocusing effect. Narrower and more distinct absorption peak of QDs after size refocusing is observed in Fig. 4 (b). The TEM image and corresponding statistics (shown in Fig.4 (c) and (e)) of the QDs synthesized with 5 minutes show a clear dual-size distribution of QDs. The TEM image also gives the clear evidence that both large and small QDs coexist, which is consistent with the dual peaks of luminescent emissions in Fig.4 (a) and calculations via a tight-binding method. (See S2 in **supporting information**) The TEM image and corresponding statistics (shown in Fig.4 (d) and (f)) of QDs with 30 minutes at 110°C show the more uniform shapes and narrower size distribution, suggesting that the thermodynamic perturbation with higher temperature and long reaction time facilitate the QDs to overcome chemical-potential well and ripen to uniform size distribution.

### 3.5 Mechanism of QDs growth

So far, it is confirmed that a dual size distribution of PbSe QDs is obtained during the early stage of growth. Then the size distribution refocuses in the further growth and ripening.<sup>19-21</sup> The growth mechanism of dual-size distributed PbSe QDs is illustrated in Fig.5. Classic size chemical-potential curve is shown in the black curve (dash line in Fig.5). Normally, after quick injection of precursor in hot solvent, precursor reagents decompose and form the supersaturated monomers that lead to nucleation. Monomers then add to existing particles, rather than form new nuclei when the particles reach the critical size ( $r_c$ ) for nucleation. Once monomer concentrations are sufficiently depleted, growth would be dominated by Ostwald

ripening.

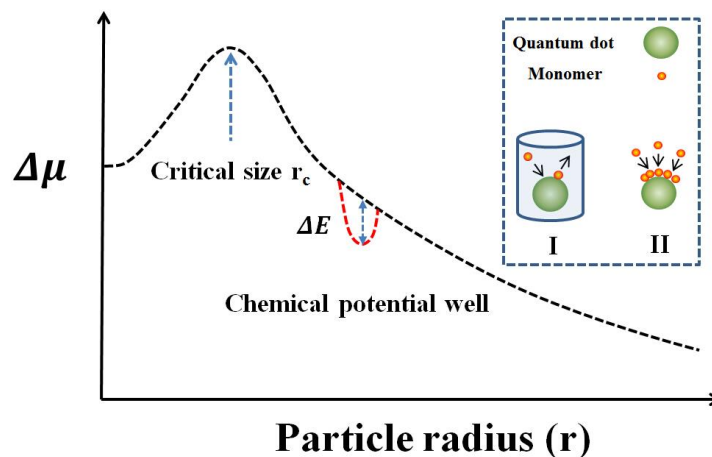


**Fig.5.** Schematic diagram for the growth mechanism of dual-size QDs

Situation can be different at the early stage of QDs growth, where the small QDs are supposed to stay in a relative low energy state, namely in an energy well (red curve) in the classic size chemical-potential curve from thermodynamic aspect. Inset of Fig.5 illustrates that the growth is suspended (Stage I) when monomers could not provide sufficient energy to overcome the chemical-potential well ( $\Delta E$ ). If extra precursors are injected (Stage II), higher concentration of monomers would initiate the growth again. The details have also been demonstrated in Section 3.3.

It should be noticed that the most important difference between the typical synthesis and the synthesis of dual size distributed PbSe QDs is the lower growth temperature. In general, the growth of IV-VI quantum dots are performed at higher temperatures above  $120^{\circ}\text{C}$ .<sup>10,22</sup> Only at a relatively low growth temperature, the QDs would be easily trapped in the chemical-potential well at the early stage of growth.<sup>8,13</sup> In this case, we assume that the dual size distribution results from the existence of ultra-small QDs which we attribute to the injection rates or incidental fluctuation in temperature during nucleation or early stage of

growth. Our experiments revealed that ultra-small QDs are more stable during relatively-low-temperature growth because of them being easily trapped in the chemical-potential well, while the larger QDs grow faster. This leads to the remarkable size separation.

Despite the successive injection of precursors (kinetic perturbation), higher growth temperature (thermodynamic perturbation) could also facilitate QDs to overcome the chemical-potential well. When the growth temperature is maintained high, system can provide enough energy that helps small QDs overcome the potential well and keep growing. Size distribution will refocus at the following stage where the small QDs grow faster than the large QDs for the monomer addition rate being scaled as the inverse of the QD radius  $R$  (rate $\sim 1/R$ ).<sup>19, 23</sup> As monomers are consumed, the average size slowly increase while the size distribution slightly broaden because of the Ostwald ripening. But this broadening is limited and won't cause a remarkable variation of size distribution.

#### 4. Conclusion

In summary, controllable synthesis and growth mechanism of dual size distributed PbSe QDs are systematically studied. Both HR-TEM images and photoluminescence emissions observed in PL spectra clearly demonstrate the co-existence of dual-size QDs. The studies of temperature variation and kinetic perturbation with successive injection of precursors verify the thermodynamic stability of QDs, suggesting a possible growth mechanism that leads to the dual size distribution. A chemical-potential well prevents the small QDs from growing while the large QDs are still growing, which causes a remarkable size separation. Further study of temporal evolution reveals the size refocusing of QDs. Both successive injections of

precursors (kinetic perturbation) and higher growth temperature (thermodynamic perturbation) can provide enough energy that facilitates small QDs to overcome the chemical-potential well. Understanding of this process is essential for the controllable synthesis and various applications of PbSe QDs.

### Acknowledgements

This work was supported by National Key Basic Research Program of China (No. 2011CB925603) and Natural Science Foundation of China (No. 61290305, 11374259, and 61275108).

### References:

1. Finlayson, C. E.; Amezcua, A.; Sazio, P.; Walker, P. S.; Grossel, M. C.; Curry, R. J.; Smith, D. C.; Baumberg, J. J. *J MOD OPTIC*. **2005**, *52*, (7), 955--964.
2. Semonin, O. E.; Luther, J. M.; Choi, S.; Chen, H. Y.; Gao, J.; Nozik, A. J.; Beard, M. C. *Science* **2011**, *334*, (6062), 1530--1533.
3. Choi, J. J.; Lim, Y. F.; Santiago-Berrios, M. B.; Oh, M.; Hyun, B. R.; Sung, L. F.; Bartnik, A. C.; Goedhart, A.; Malliaras, G. G.; Abruna, H. D.; Wise, F. W.; Hanrath, T. *Nano Lett.* **2009**, *9*, (11), 3749-3755.
4. Miehalet, X.; Pinaud, F. F.; Bentolila, L. A.; Others. *Vivo Imaging, and Diagnostics* **2005**, *307*, (5709), 538--544.
5. Trinh, M. T.; Houtepen, A. J.; Schins, J. M.; Hanrath, T.; Piris, J.; Knulst, W.; Goossens, A.; Siebbeles, L. *Nano Lett.* **2008**, *8*, (6), 1713-1718.
6. Trinh, M. T.; Polak, L.; Schins, J. M.; Houtepen, A. J.; Vaxenburg, R.; Maikov, G. I.

Grinbom, G.; Midgett, A. G.; Luther, J. M.; Beard, M. C.; Nozik, A. J.; Bonn, M.; Lifshitz, E.; Siebbeles, L. *Nano Lett.* **2011**, 11, (4), 1623-1629.

7. Ma, W.; Swisher, S. L.; Ewers, T.; Engel, J.; Ferry, V. E.; Atwater, H. A.; Alivisatos, A. *P. ACS Nano* **2011**, 5, (10), 8140--8147.

8. Evans, C. M.; Guo, L.; Peterson, J. J.; Maccagnano-Zacher, S.; Krauss, T. D. *Nano Lett.* **2008**, 8, (9), 2896--2899.

9. Murray, C. B.; Sun, S.; Gaschler, W.; DoyLe, H.; Betley, T. A.; Kagan, C. R. *IBM J. Res. Dev.* **2001**, 45, (1), 47--56.

10. Yu, W. W.; Falkner, J. C.; Shih, B. S.; Colvin, V. L. *Chem. Mater.* **2004**, 16, (17), 3318-3322.

11. Ouyang, J. Y.; Schuurmans, C.; Zhang, Y. G.; Nagelkerke, R.; Wu, X. H.; Kingston, D.; Wang, Z. Y.; Wilkinson, D.; Li, C. S.; Leek, D. M.; Tao, Y.; Yu, K. *ACS Appl. Mater. Inter.* **2011**, 3, (2), 553-565.

12. LaMer, V. K.; Dinegar, R. H. *J. Am. Chem. Soc.* **1950**, 72, (11), 4847--4854.

13. Kudera, S.; Zanella, M.; Giannini, C.; Rizzo, A.; Li, Y.; Gigli, G.; Cingolani, R.; Ciccarella, G.; Spahl, W.; Parak, W. J.; Manna, L. *Adv. Mater.* **2007**, 19, (4), 548-552.

14. Hu, L.; Wu, H. Z.; Cai, C. F.; Xu, T. N.; Zhang, B. P.; Jin, S. Q.; Wan, Z. F.; Wei, X. D. *J. Phys. Chem. C* **2012**, 116, (20), 11283-11291.

15. Hu, L.; Wu, H.; Zhang, B.; Du, L.; Xu, T.; Chen, Y.; Zhang, Y. *Small* **2014**, 10, (15), 3099-3109.

16. Yang S.; Brian K.; William Y.W.; Shang S.; Cao B; Zeng H.; Zhao Y.; Li W.; Liu Z.; Cai W.; Tony J.H. *Adv. Mater.* **2012**, 24, (41), 5598--5603

17. Trinh, M. T.; Houtepen, A. J.; Schins, J. M.; Piris, J.; Siebbeles, L. D. A. *Nano Lett.* **2008**, 8, (7), 2112--2117.
18. Trinh, M. T.; Sfeir, M. Y.; Choi, J. J.; Owen, J. S.; Zhu, X. *Nano Lett.* **2013**,
19. Peng, X. G.; Wickham, J.; Alivisatos, A. P. *J. Am. Chem. Soc.* **1998**, 120, (21), 5343-5344.
20. Chen, Y.; Johnson, E.; Peng, X. *J. Am. Chem. Soc.* **2007**, 129, (35), 10937-47.
21. Johnson, N. J.; Korinek, A.; Dong, C.; van Veggel, F. C. *J. Am. Chem. Soc.* **2012**, 134, (27), 11068-71.
22. Sarasqueta, G.; Choudhury, K. R.; So, F. *Chem. Mater.* **2010**, 22, (11), 3496-3501.
23. Sowers, K. L.; Swartz, B.; Krauss, T. D. *Chem. Mater.* **2013**, 25, (8), 1351--1362.